SMAR 2015 – Third Conference on Smart Monitoring,
Assessment and Rehabilitation of Civil Structures

SMAR 2015

Modeling of Coupled Nonlinear Shear and Flexural Responses in Medium-Rise RC Walls

Burak HOROZ[1], M.Fethi GÜLLÜ[2], and Kutay ORAKÇAL[3]

[1] Research Assistant, Bogazici University, Istanbul, Turkey
[2] Research Assistant, Bogazici University, Istanbul, Turkey
[3] Associate Professor, Bogazici University, Istanbul, Turkey

ABSTRACT: A macroscopic finite element modeling approach was adopted in this study for simulating the in-plane hysteretic lateral load behavior of medium-rise reinforced concrete structural walls, with coupled nonlinear flexural and shear response components. The behavioral characteristics of the constitutive panel elements incorporated in the model formulation are based on a fixed-crack-angle modeling methodology. Improvements are made on the constitutive panel model formulation, for better representation of the shear-aggregate-interlock effects in concrete and dowel action on reinforcing bars, constituting the shear stress transfer mechanisms across the cracks. The model formulation was implemented into MATLAB and analyses were performed using a drift-controlled nonlinear analysis solution strategy. The model was extensively calibrated for five heavily-instrumented wall specimens with moderate aspect ratios (1.5 and 2), and model predictions were compared with experimentally-measured responses. Response comparisons revealed that the model provides reasonable predictions of the lateral load capacity, stiffness degradation, hysteretic shape, ductility, and pinching characteristics of the wall specimens investigated. The model also provides reasonably accurate estimates of the relative contribution of flexural and shear deformations to wall displacements, longitudinal strain profiles along the base of the wall, and crack orientations. The modeling approach implemented in this study is believed to be a significant improvement towards reliable prediction of the coupled shear-flexural response of reinforced concrete walls under cyclic loading conditions.

1 INTRODUCTION

Reinforced concrete structural walls provide significant contribution to resisting the earthquake effects on building-type structures. Under service earthquakes, they are expected to provide sufficient stiffness and lateral load capacity to limit the lateral displacement demand on buildings, without significant damage. Under severe (design or maximum considered) earthquake actions, walls are designed and detailed to possess the required ductility characteristics and dissipate hysteretic energy without significant reduction in the lateral load capacity of the structure. Since structural walls are utilized as the main lateral load resisting members in numerous building systems, vast amount of research has been conducted to characterize the seismic behavior of structural walls. In terms of behavioral characteristics under lateral loads, the structural walls are classified into 3 groups, depending on their aspect ratios. The behavior of squat structural walls with aspect ratios less than 1.0–1.5 are controlled by shear, whereas relatively slender structural walls with aspect ratios exceeding 2.5–3.0 are predominantly controlled by flexural actions. For structural walls with moderate aspect ratios (between 1.5 and 2.5), both flexural yielding and nonlinear shear deformations (which are usually coupled) contribute to wall behavior. For such walls, nonlinear shear deformations can

constitute 30% to 50% of wall lateral displacements, as investigated experimentally by Tran and Wallace (2012). Reliable behavioral modeling of such structural walls with predominant shear-flexure interaction behavior is of particular interest, especially because fiber-based modeling methodologies commonly used in practice for performance-based design of buildings typically consider uncoupled shear and flexural response components, which fails to represent the experimentally-observed response characteristics of walls on which shear demands are significant.

The Multiple-Vertical Line Element Model (MVLEM) proposed by Vulcano et al. (1988) is one of the pioneering fiber-based modeling approaches to represent the nonlinear flexural behavior of structural walls. The formulation of this method was simplified by Fischinger (1990) via adopting force-deformation relationships instead of stress-strain relationships. Orakçal (2004) has implemented more comprehensive constitutive relationships in the model formulation. However, all of these fiber-based modeling methodologies are incapable of representing nonlinear shear-flexure interaction behavior, which can be observed even in slender walls designed to yield in flexure prior to reaching shear capacity. Studies by Orakçal and Wallace (2006) have shown that fiber models neglecting shear-flexure coupling do not correctly predict compressive strains developing in slender walls, although the global response characteristics can be captured. Moreover, fiber-based models fail to represent the lateral load behavior of moderate-aspect-ratio walls (Tran, 2012) and squat walls (Massone et al., 2006). An empirical modeling approach was proposed by Beyer et al. (2011) for simulating nonlinear shear flexure interaction in walls. Panagiotou et al. (2011) also presented an alternative method to model shear flexure interaction, using the strut-and-tie approach. As well, methodologies that are based on replacing the fibers of a fiber model with two-dimensional panel elements have been proposed (e.g. Massone et al. 2006, 2009; Fischinger et al., 2012; Jiang and Kurama, 2010; Kolozvari et al., 2012). However, most of the modeling approaches available in the literature incorporate various assumptions and simplifications, and are subject to limitations. There is still a need for a reliable and generalized, yet relatively simple modeling approach that can simulate the coupled flexural and shear responses of walls with various geometries and aspect ratios.

In this study, a relatively simple yet robust finite element modeling approach was adopted for simulating the in plane behavior of structural walls with moderate aspect ratios (1.5 and 2.0), under reversed cyclic loading conditions. The Fixed-Strut-Angle-Model (FSAM), originally proposed by Uluğtekin (2010), was adopted as the constitutive reinforced concrete panel (membrane) element in the two-dimensional finite element model formulation. Simple behavioral models representing dowel action and aggregate interlock mechanisms were incorporated in the panel model formulation for transfer of shear stresses across crack surfaces. Analytical model predictions were obtained for five heavily-instrumented medium-rise wall specimens tested by Tran and Wallace (2012), which have experienced flexural yielding coupled with nonlinear shear deformations. Model predictions were compared with experimental data at both global (force-displacement) and local (deformation) response levels.

2 ANALYTICAL MODEL DESCRIPTION

Rectangular four-node constitutive panel (membrane) elements were used for two-dimensional finite element modeling of structural walls. The finite element model formulation was constructed via assembly of the panel elements. The behavior of the reinforced concrete panel elements incorporate hysteretic stress–strain behavior for concrete and reinforcing steel, as well as other behavioral characteristics including compression softening, tension stiffening, hysteretic biaxial damage on concrete, shear aggregate interlock along crack surfaces, and

dowel action on the reinforcing bars. The so-called Fixed-Strut-Angle-Model (FSAM), originally proposed by Uluğtekin (2010), was adopted as the base model for the panel elements. However, the formulation of the FSAM was improved to incorporate shear aggregate interlock and dowel action effects for transfer of shear stresses across cracks. The base assumption in the original FSAM is that crack directions coincide with principal stress directions in concrete, implying zero shear stress developing along the crack surface. After cracking, principal stress directions in concrete are fixed along the fixed strut (crack) directions, whereas principal strain directions are free to rotate. The behavior of concrete along the fixed compression struts within each panel element is represented using biaxial stress–strain relationships, whereas the behavior of reinforcing steel is described by uniaxial stress-strain relationships applied along the directions of reinforcing steel bars. The hysteretic stress–strain relationship for concrete by Chang and Mander (1994) is adopted in the model formulation (Figure 1a), also considering biaxial compression softening and biaxial hysteretic damage effects. The reinforcing steel stress–strain relationship proposed by Menegetto and Pinto (1973) is used to represent uniaxial hysteretic behavior of reinforcing bars (Figure 1b).

Prior to formation of the first crack in the FSAM, the stress–strain behavior of concrete is assumed to follow the monotonic envelope. It is assumed that the principal stress and strain directions coincide, and the stress–strain model for concrete is applied in the principal strain direction in a rotating manner (Figure 2a). When the principal tensile strain first exceeds the monotonic cracking strain of concrete, the first crack forms in the FSAM, in perpendicular direction to the principal tensile strain. Thereby the first fixed strut develops, which is parallel to the direction of the first crack. The direction of the first strut (crack) remains constant during later loading stages, where the principal strain directions continue to rotate, whereas the principal stress directions, along which the concrete stress–strain relationship is applied, are fixed (Figure 2b).

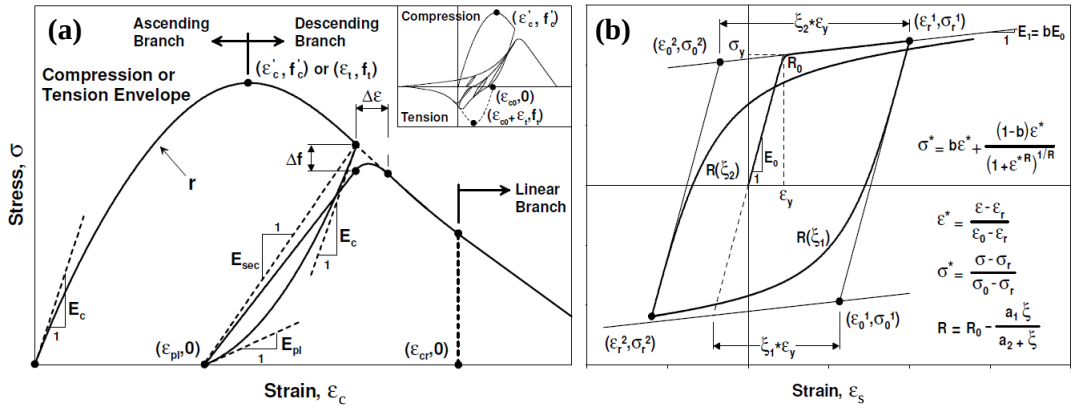

Figure1. Material constitutive models: (a) Concrete, (b) Reinforcing steel.

As principal concrete stress and crack directions are assumed to coincide, no shear stress develops along the crack directions, implying zero aggregate interlock and zero dowel action assumptions in the base (original) formulation of the FSAM. This also implies that the second crack has to develop in perpendicular direction to the first crack. Before formation of the second crack, the stress–strain relationship is applied in parallel and perpendicular directions to the first crack, in the form of a single strut mechanism. When the tensile strain along the first strut exceeds the cracking strain of concrete, the second crack (and strut) develops perpendicular to the first crack direction. The biaxial behavior of concrete after formation of the second crack is

shown in Figure 2c. During further stages of loading, these two struts are subjected to tension or compression, and the concrete stress–strain model is applied along the two fixed strut (fixed principal stress) directions. The stress in the reinforcing steel bars is calculated using the uniaxial stress–strain relationship along the bar directions. The stresses developing in concrete and reinforcing steel bars are then superimposed (considering the reinforcement ratios) to obtain the average (smeared) stresses developing in the reinforced concrete panel element.

The original formulation of the FSAM, in which the aggregate interlock and the dowel action mechanisms are ignored, was later modified since the assumption that no shear stress transfer occurs across crack surface may lead to overestimation of shear deformations and prediction of premature sliding shear failures. To remedy this shortcoming of the original FSAM, Orakçal et al. (2012) proposed a simple friction-based elasto-plastic aggregate interlock model, generating sliding shear stresses on crack surfaces (Figure 3b). In this interlock model, when the normal stress perpendicular to the crack surface is tensile, the sliding stress effect is assumed to be zero. When the normal stress perpendicular to the crack surface is compressive, the sliding shear stress is bounded by the product of that compressive stress and a shear friction coefficient (e.g., μ_c=1.0). Güllü and Orakcal (2014) also considered the clamping effect of reinforcing steel bars straddling the crack surface to the sliding shear stress (shear friction) capacity of the aggregate interlock model, similarly to the approach presented in ACI-318-11 (Figure 3a).

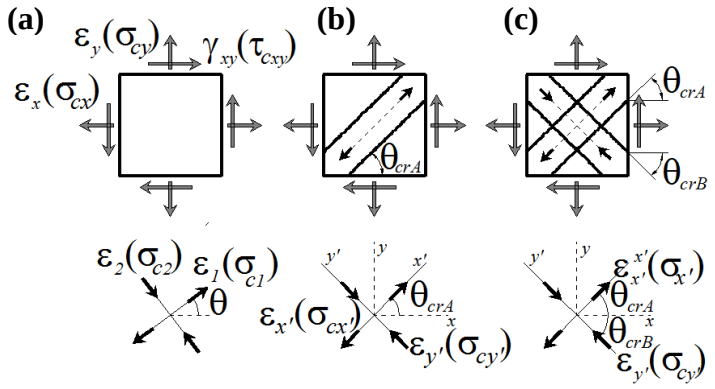

Figure 2. Fixed Strut Angle Model (FSAM) – concrete behavior (a) Uncracked behavior, (b) Behavior after formation of first crack, (c) Behavior after formation of second crack (Kolozvari et al., 2014).

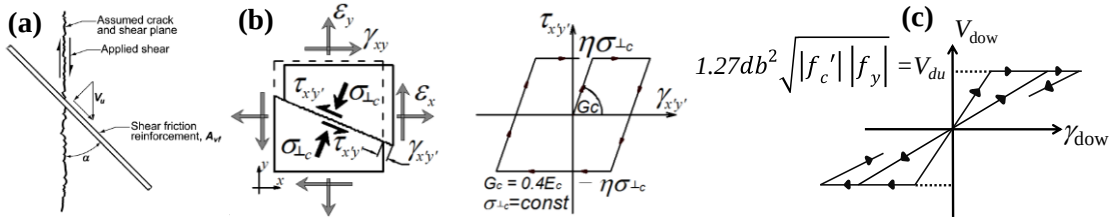

Figure 3. a) Shear-friction mechanism along a crack in ACI-318, b) Friction-based constitutive model for shear aggregate interlock (Orakcal et al., 2012), c) Dowel action model.

In this study, dowel action effects on the vertical reinforcing steel bars in a structural wall are also incorporated in the formulation of the FSAM. The elasto-plastic dowel action model presented by He and Kwan (2001) is implemented as the monotonic envelope of the dowel force – shear strain constitutive relationship, and origin-oriented unloading and reloading paths are

adopted to represent hysteretic behavior (Figure 3c). The shear aggregate interlock mechanism in the present model formulation is represented via a similar approach to Güllü and Orakçal (2014). However, contribution of the clamping force created by the reinforcing steel bars to the shear friction capacity is represented by a friction coefficient of μ_s=0.5, whereas contribution of the compressive stress in concrete perpendicular to the crack surface is considered using a friction coefficient of μ_c=1.0. As well, while the sliding shear stresses on the crack surface resulting from the compressive stress in concrete follows elasto-plastic hysteretic behavior (Figure 3b), those resulting from the clamping force of the reinforcing steel bars are assumed to follow an origin-oriented hysteretic behavior. These modeling approaches for transfer of shear stress across cracks were all developed considering available literature on the subject, as well as prior test observations.

3 COMPARISON OF MODEL RESULTS AND TEST RESULTS

For experimental validation of the model, test results on 5 medium-rise wall specimens tested by Tran and Wallace (2012) were used. The specimens are characterized by their aspect ratios (1.5 and 2.0), axial load levels ($0.025A_g f_c'$ and $0.10A_g f_c'$), and reinforcement configurations at boundary and web regions. Table 1 summarizes the geometry and reinforcement details for all 5 wall specimens. Concrete with compressive strength of 34.5 MPa and boundary reinforcement with yield strength of 414 MPa were used for all specimens. The walls were tested under reversed cyclic lateral loads, while the axial loads on the specimens were kept constant.

Table 1. Geometry and reinforcement details for the wall sprecimens.

	Specimen	Height (cm)	Width (cm)	Aspect Ratio	$P_{ax}/A_g f_c'$	Web Reinforcements		Boundary Reinforcements	
						Reinforcement	$\rho_l = \rho_t$ (%)	Reinforcement	ρ_b (%)
Tran and Wallace (2012)	RW-A20-P10-S38	244	122	2.0	0.10	6.00 mm @ 140 mm	0.27	8 x 12.70 mm	3.23
	RW-A20-P10-S63	244	122	2.0	0.10	9.53 mm @ 152 mm	0.61	8 x 19.05 mm	7.11
	RW-A15-P10-S51	183	122	1.5	0.10	6.00 mm @ 114 mm	0.32	8 x 12.70 mm	3.23
	RW-A15-P10-S78	183	122	1.5	0.10	9.53 mm @ 127 mm	0.73	4 x 19.05 mm 4 x 15.87 mm	6.06
	RW-A15-P2.5-S64	183	122	1.5	0.025	9.53 mm @ 152 mm	0.61	4 x 19.05 mm 4 x 15.87 mm	6.06

The analytical model was calibrated to represent the geometric and material properties of the test specimens, as well as the loading conditions. Model predictions were compared with test results both at global (lateral load–displacement, Figure 4) and local (deformations, Figure 5) response levels for all specimens. The local response comparisons presented in this paper include flexural and shear deformation contributions to lateral displacement, vertical growth, average rotations, longitudinal strain profiles, and crack orientations, only for selected specimens.

For specimens RW-A20-P10-S38 and RW-A15-P10-S51, lateral strength degradation (failure) initiated with crushing of core concrete in wall boundaries and buckling of longitudinal boundary reinforcement. Strength degradation due to widening of the diagonal cracks was also observed during the tests. As shown in Figures 4a and Figure 4c, the analytical model results are in agreement with the test results for these two specimens, in terms of lateral load capacity and ductility, as well as wall other important response characteristics such as stiffness degradation, plastic deformations, pinching, and contribution of shear deformations to lateral displacements at the top of the walls.

The model also provides a reasonable response prediction for specimen RW-A20-P10-S63, which experienced strength degradation due to the crushing of concrete starting from the base of

the wall and propagating along diagonal compression struts. As shown in Figure 4b, the model provides very close estimations for the contribution of shear deformations to lateral displacement of this specimen. For specimens RW-A15-P10-S78 and RW-A15-P2.5-S64, which experienced failure due to crushing of the diagonal compression strut at wall base, model predictions presented in Figures 4e and 4d are again reasonable. However, distinctively for specimen RW-A15-P2.5-S64, the model fails to accurately capture the pinching behavior in the lateral load–displacement response, as well as the contribution of shear deformation to wall lateral displacements (Figure 4e). This specimen was subjected a very low axial load level, and experienced unexpected formation of a premature horizontal crack close to the bottom of the wall (along a horizontal rebar in the wall web), resulting in sliding shear behavior along that horizontal crack, which could not be predicted by the model. Figure 4f compares test results and model estimations for the contribution of shear deformations to lateral displacements at the top of the specimens (average of all drift levels). Overall, with the exception of specimen RW-A15-P2.5-S64 which suffered premature sliding shear failure, the model provides reasonably accurate predictions for lateral load–displacement responses and contribution of shear deformations to wall displacements.

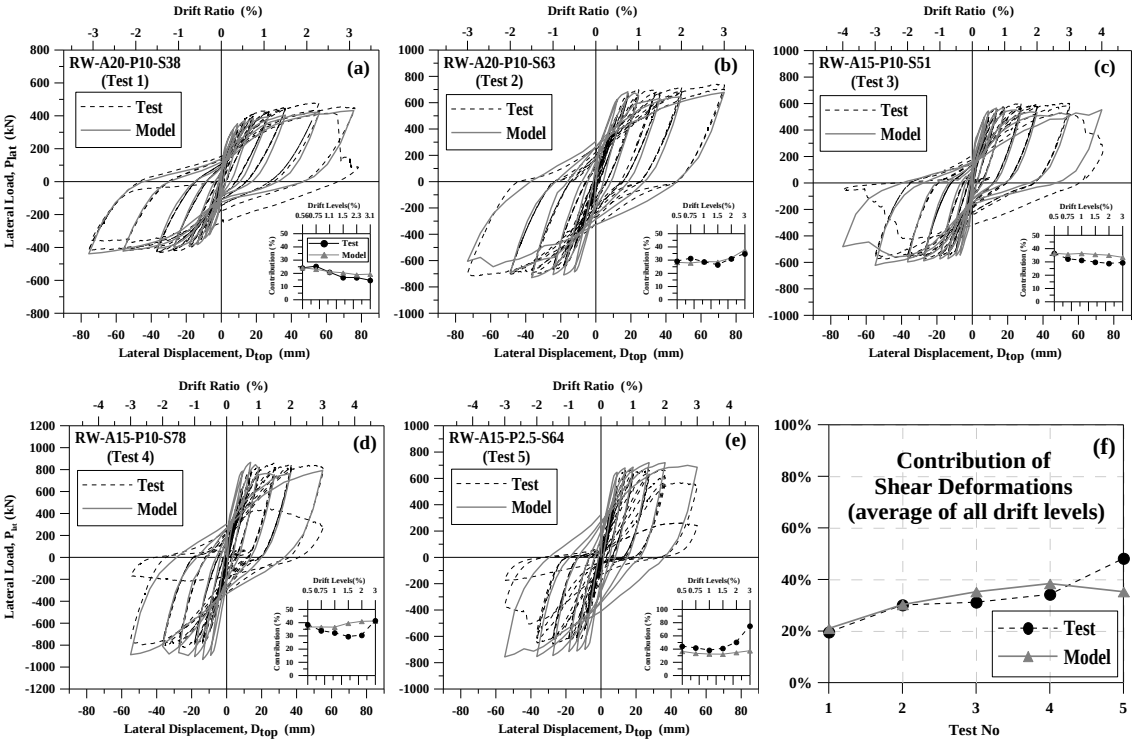

Figure 4. Lateral load vs. top displacement responses for a) RW-A20-P10-S38, b) RW-A20-P10-S63, c) RW-A15-P10-S51, d) RW-A15-P10-S78, e) RW-A15-P2.5-S64; f) Contribution of shear deformations to lateral displacements at the top of the walls.

Analytical model predictions were compared with test results at also local (deformation) response levels. It is shown in Figures 5a and 5b that the model can successfully simulate the lateral load vs. flexural and lateral load vs. shear deformation response characteristics for specimen RW-A15-P10-S51. Figures 5d and 5e illustrate that the model captures the profile (distribution) of the lateral flexural and shear displacements along the height of specimens RW-A20-P10-S38 and RW-A20-P10-S63 at various applied drift levels. Figure 5c depicts that the

vertical displacement at the top of the wall (vertical growth) vs. lateral displacement relationship is also captured for specimen RW-A15-P10-S78, indicating that the model is successful in predicting the yielding of the longitudinal wall reinforcement and migration of the neutral axis. In Figure 5f, the experimentally-observed crack pattern on specimen RW-A15-P10-S78 at a drift ratio of 2.0% is compared with the crack directions predicted by the model, demonstrating reasonable agreement. It is shown in Figure 5g that the model can reasonably capture the rotations along the expected plastic hinge region of specimen RW-A20-P10-S63 at various drift levels. Measured and predicted vertical strain profiles (along the wall cross section) at the bottom of specimen RW-A20-P10-S63 are compared in Figure 5h at various drift levels. The model provides reasonably accurate predictions of both compressive and tensile strains, as well as the location of the neutral axis on the wall cross section.

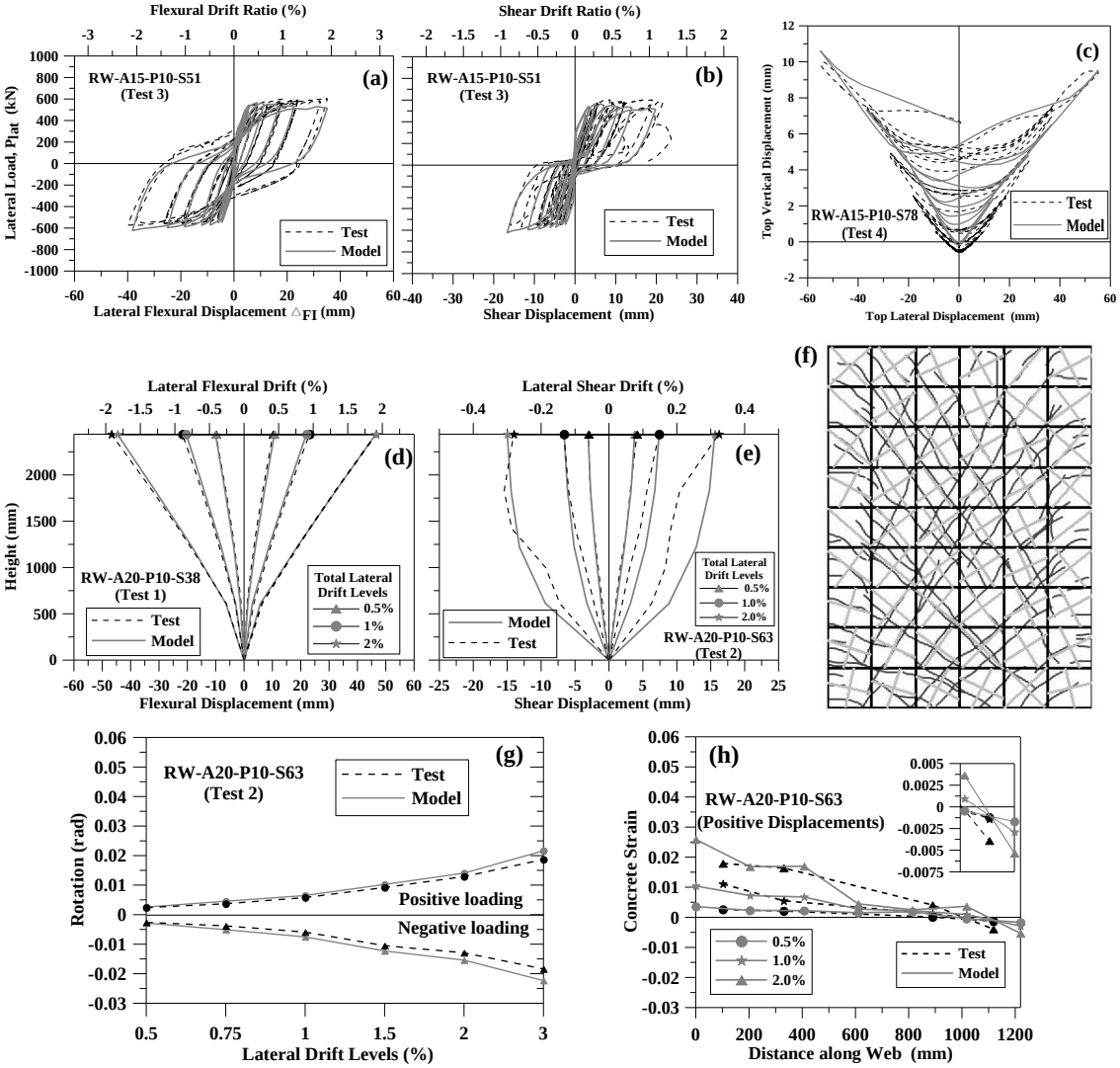

Figure 5. a) Lateral load vs. top flexural displacement for Test 3, b) Lateral load vs. top shear displacement for Test 3, c) Vertical growth vs. top lateral displacement for Test 4, d) Flexural displacement profile for Test 1, e) Shear displacement profile for Test 2, f) Crack directions for Test 4 at

2.0% drift (analytical is gray and experimental is black), g) Plastic hinge rotations for Test 2, h) Vertical strain profile for Test2.

4 RESULTS

A simple finite element modeling approach was adopted in this study for simulating the in-plane hysteretic lateral load behavior of medium-rise reinforced concrete structural walls, with coupled nonlinear flexural and shear response components. Response comparisons with test results on medium-rise wall specimens revealed that the model provides reasonable predictions of the lateral load capacity, stiffness degradation, hysteretic shape, ductility, and pinching characteristics of the walls. The model also provides reasonably accurate estimates of the relative contribution of flexural and shear deformations to wall displacements, wall rotations, longitudinal strain profiles along the base of the wall, and crack directions. For better prediction of the response of walls experiencing sliding shear failure, ongoing efforts focus on incorporating more robust constitutive models to represent shear aggregate interlock and dowel action mechanisms.

5 ACKNOWLEDGEMENTS

The authors would like to thank Prof. John W. Wallace and Dr. Thien Tran from UCLA and Prof. Kristijan Kolozvari from California State University Fullerton for sharing the test data.

6 REFERENCES

Belarbi, A. and T. C. Hsu, 1994, "Constitutive Laws of Concrete in Tension and Reinforcing Bars Stiffened By Concrete", ACI Structural Journal, Vol. 91, No. 4, pp. 465-474.

Chang G A and Mander, J B, 1994, Seismic Energy Based Fatigue Damage Analysis of Bridge columns: Part I – Evaluation of Seismic Capacity, NCEER Technical Report, State University of New York, Buffalo, NY.

Güllü M F, 2013, Finite Element Modeling Reinforced Concrete Structural Walls, MS. Thesis, Boğaziçi University.

Güllü M F and K Orakçal, 2014, "Nonlinear Finite Element Modeling of Reinforced Concrete Structural Walls", Proceedings, 2nd European Conference on Earthquake Engineering and Seismology, İstanbul, Türkiye, No. 1485.

He X G and Kwan A K H, 2001, "Modeling Dowel Action of Reinforcement Bars for Finite Element Analysis of Structures", Computers and Structures, Vol.79, Issue 6, pp. 595-604.

Kolozvari K, Tran T, Orakcal K and Wallace J, 2014, "Modeling of Cyclic Shear-Flexure Interaction in Reinforced Concrete Structural Walls II: Experimental Validation",Journal of Structural Engineering, 10.1061/(ASCE)ST.1943-541X.0001083 , 04014136.

Menegotto M and Pinto E, 1973, "Method of Analysis for Cyclically Loaded Reinforced Concrete Plane Frames",IABSE Symposium on Resistance and Ultimate Deformability of Structures Acted on by Well-Defined Repeated Loads. Lisbon, Portugal.

Orakçal K ,2004, Nonlinear Modeling and Analysis of Slender Reinforced Concrete Walls, Ph.D. Thesis, University of California.

Orakçal K, D Ulugtekin and L M Massone, 2012, "Constitutive Modeling of Reinforced Concrete Panel Behavior under Cyclic Loading" Proceedings, 15th World Conference on Earthquake Engineering, Lisbon, Portugal, No. 3573.

Tran T A, 2012, Experimental and Analytical Studies of Moderate Aspect Ratio Reinforced Concrete Structural Walls, Phd. Thesis, University of California

Tran T A and Wallace J W, 2012, "Experimental Study of Nonlinear Flexural and Shear Deformations of Reinforced Concrete Structural Walls" Proceedings, 15th World Conference on Earthquake Engineering, Lisbon, Portugal. ,

Uluğtekin D, 2010, Analytical Modeling of Reinforced Concrete Panel Elements under Reversed Cyclic Loadings, MS. Thesis, Boğaziçi University.